Comparison of Langmuir and emissive probes as diagnostics for turbulence studies in the low-temperature plasma of the torsatron TJ-K

2005 Plasma Phys. Control. Fusion 47 569

(http://iopscience.iop.org/0741-3335/47/4/001)

INSTITUTE OF PHYSICS PUBLISHING PLASMA PHYSICS AND CONTROLLED FUSION

Plasma Phys. Control. Fusion **47** (2005) 569–579 doi:10.1088/0741-3335/47/4/001

Comparison of Langmuir and emissive probes as diagnostics for turbulence studies in the low-temperature plasma of the torsatron TJ-K

N Mahdizadeh[1], F Greiner[1], M Ramisch[1], U Stroth[1], W Guttenfelder[2], C Lechte[1] and K Rahbarnia[1]

[1] IEAP, University of Kiel, 24098 Kiel, Germany
[2] HSX Plasma Laboratory, University of Wisconsin-Madison, USA

E-mail: zadeh@physik.uni-kiel.de

Received 24 September 2004, in final form 6 January 2005
Published 4 March 2005
Online at stacks.iop.org/PPCF/47/569

Abstract

For the investigation of turbulent transport in magnetized plasmas, the cross-phase between density and plasma potential fluctuations is a key parameter. In the majority of the experimental studies, the floating potential of a conventional Langmuir probe is used as an estimate for the plasma potential. It is well known, however, that plasma and floating potential fluctuations can have different phases if temperature fluctuations are present in the plasma. A diagnostic giving a direct estimate of the plasma potential fluctuations is the emissive probe. In this work, potential measurements from both emissive and Langmuir probes are directly compared. The experiments are carried out in the magnetically confined low-temperature plasma of the TJ-K torsatron. Potential, electric field and density fluctuations are measured with a three-tip probe array in the entire plasma volume. Profiles of mean values and fluctuations of the parameters are compared. The deviation of the mean plasma potential from the floating potential is larger than expected from simple probe theory. The measurements of fluctuations, however, which are relevant for turbulence studies, do not show a significant difference. This justifies the use of Langmuir probes for turbulence studies at least in toroidal low-temperature plasmas.

1. Introduction

In order to investigate coherent structures or turbulent transport in a plasma, the phase between plasma potential and density fluctuations is a crucial quantity. It is indicative of the turbulence driving mechanism and determines the level of radial transport. Although Langmuir probes give only an indirect measure of the plasma potential, they are applied in virtually all fluctuation

measurements and the floating potential is interpreted as if it was the plasma potential (see [1–6] and citations therein). The reason for this is that Langmuir probes are much more robust and easier to handle than emissive probes. It is well known, however, that due to temperature fluctuations the fluctuations in floating potential can significantly deviate from those in plasma potential. As a consequence, the use of floating potential measurements in turbulence studies has to be legitimated for each experimental condition individually.

In high-temperature plasmas like in fusion devices, this can be done by means of fast (>1 MHz) swept Langmuir probes, which allow the measurement of time-resolved temperature fluctuations. Such experiments have been carried out in the stellarator W7-AS [7]. For low-temperature plasmas, emissive probes can be used to measure the plasma potential directly [8]. Emissive probes have a probe tip, which is heated up to thermionic electron emission. The heating can be done with an electric current through the probe or indirectly, e.g. by high-power laser [9]. Due to the high heat load in fusion plasmas, the use of emissive probes is restricted to the plasma edge where the difference between mean plasma and floating potentials has already been investigated in [10] where it has been shown that simple probe theory is not sufficient to explain the difference between the two quantities. Recently, emissive probes have been tested as a fluctuation diagnostic in the edge of smaller tokamaks [11].

It is still an unresolved issue as to what extent an emissive probe measures the plasma potential. A virtual cathode around the probe tip can move the floating potential away from the plasma potential [12]. The size of this effect is not well established yet. Our comparison of cold and emissive probe characteristics indicates that, for the parameters of the TJ-K plasma, the floating potential of the emissive probe is close to the plasma potential. For the sake of a clearer presentation, the floating potential of the emissive probes here will be referred to as 'plasma potential'.

This work concentrates on a comparative study of turbulent transport measurements carried out with Langmuir and emissive probes in the entire poloidal cross-section of the low-temperature plasma of the torsatron TJ-K [6, 13]. On this device, extensive turbulence studies have been carried out previously by means of Langmuir probes [14, 15]. In order to assess potential errors which might be introduced by using floating instead of plasma potential, the following questions are addressed: (i) How do the background floating and plasma potentials, Φ_{F} and Φ_{P}, respectively, compare and can the observed difference be explained in terms of the measured electron temperature T_{e}? (ii) What is the influence of an emissive probe on measurements of the ion saturation current by an adjacent Langmuir probe in a typical setup used for transport studies? (iii) What is the difference between fluctuations in the two potential measurements $\tilde{\Phi}_{\mathrm{F}}$ and $\tilde{\Phi}_{\mathrm{P}}$ and what is their phase with respect to the ion saturation current fluctuations $\tilde{I}_{\mathrm{i,sat}}$?

The paper is organized as follows. After presentations of experiment and probe system in section 2, equilibrium profiles obtained by Langmuir and emissive probes and a study of the influence of the emissive probes on the plasma equilibrium are presented in section 3. Section 4 is dedicated to the comparison of potential and electric field fluctuation measurements and in section 5 the conclusions are drawn.

2. Experimental set-up

TJ-K is a small-size torsatron with a major radius of $R_0 = 0.6\,\mathrm{m}$ and a minor radius of $a = 0.1\,\mathrm{m}$ and a rotational transform of about $\frac{1}{3}$. Due to plasma generation by electron cyclotron resonance heating (ECRH) at 2.45 GHz, the nominal magnetic field is limited to the range $B = 70$–$100\,\mathrm{mT}$. Experiments have been carried out on continuous discharges of about 30 min duration. Further information on the operation parameter can be found in [6, 15]. In the

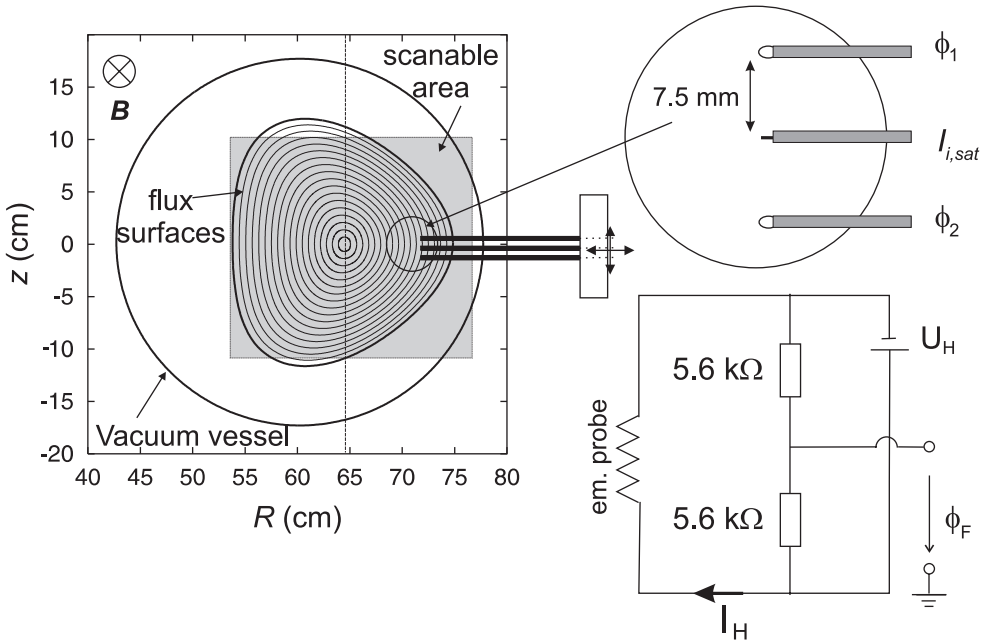

Figure 1. Schematic drawing of the transport probe and the electric circuit of the emissive probes. The transport probe consists of a cylindrical Langmuir probe in the centre sandwiched between two emissive probes. The central tip measures $I_{\mathrm{i,sat}}$, the two outer probes the plasma potential Φ_{P} (emissive) or the floating potential Φ_{F} (cold). The vertical distance between adjacent probes is 7.5 mm. On the lower right, the electrical circuit is depicted, consisting of a power supply for the heating current and a network of two resistors, which shifts the reference point for the potential measurement to the centre of the tungsten loop.

present experiments, the working gas was argon at a neutral gas pressure of $P_0 = 5 \times 10^{-5}$ mbar and a heating power of 2 kW. The electron temperature was $T_{\mathrm{e}} \simeq 10$ eV and the line-average density about $1.2 \times 10^{17}\,\mathrm{m}^{-3}$.

In order to study turbulent transport,

$$\tilde{\Gamma}_r \sim \tilde{n}\tilde{E}_\theta, \tag{1}$$

the fluctuations in density $\tilde{n}$ and poloidal electric field $\tilde{E}_\theta$ have to be measured simultaneously. This has been achieved with the *transport probe* depicted in figure 1. It consists of a central Langmuir probe sandwiched between two emissive probes in a distance of $d = 7.5$ mm. As density measurement, the ion saturation current $I_{\mathrm{i,sat}}$ of the central Langmuir probe is used, built out of a 0.2 mm diameter tungsten wire insulated in a 2.7 mm alumina tube. The probe tip has a length of 3 mm and is connected with short cables via a resistor of 1 kΩ to a battery with a voltage of −90 V. The two outer emissive probes are constructed of a 0.1 mm diameter tungsten wire that forms a loop of about 2 mm diameter connected to two 0.3 mm diameter copper wires embedded in a 2.7 mm alumina tube with two bores. The technical design of the probes is similar to that given in [16], the copper wire is twisted around the tungsten wire and squeezed into the alumina tube. These probes are operated in two modes referred to as *cold* and *emissive*. In the cold mode they act as Langmuir probes and measure the floating potential while the floating potential measured in the emissive mode, obtained by heating with an external current through the loop, is interpreted as the plasma potential. The loop was oriented perpendicular to the magnetic field. Figure 1 also shows the electrical circuit consisting of a power supply

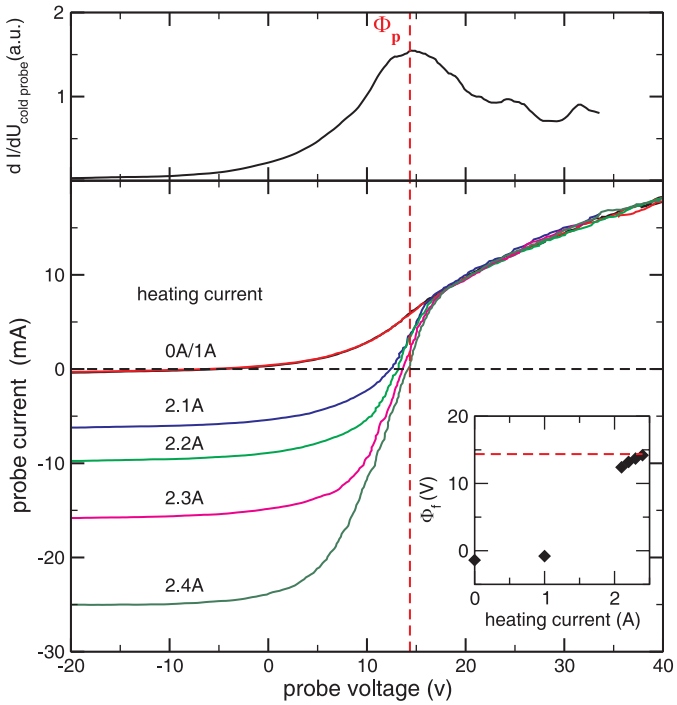

Figure 2. Current–voltage characteristic of an emissive probe for different heating currents I_H as indicated in the figure. The inserted graph shows that the floating potential approaches the plasma potential with increasing heating current. The plasma potential is determined by the maximum of the slope of the cold probe characteristics, as depicted in the upper part. Data are from a helium discharge ($B = 90$ mT, $P_0 = 5 \times 10^{-5}$ mbar) at $R - R_0 = 7$ cm, the acquisition time for each characteristics was 2 s.

(This figure is in colour only in the electronic version)

for the heating current and a network of two resistors, which shifts the reference point for the potential measurement to the centre of the tungsten loop, where strongest emission due to highest temperature is assumed. The poloidal electric field at the position of the central Langmuir probe is then calculated from the signals of the outer probes according to

$$\tilde{E}_\theta = \frac{\tilde{\phi}_2 - \tilde{\phi}_1}{2d}. \tag{2}$$

Figure 2 depicts the characteristics of an emissive probe for different probe temperatures, which are set by the heating current. Increasing the heating current through the probe leads to a shift of its floating potential towards the plasma potential, determined by the maximum of the slope of the cold probe characteristics. This good agreement is in variance with previous observations, where the floating potential of the emissive probe has been found to be below the plasma potential. The difference between the true plasma potential and floating potential of a sufficiently emissive probe has been attributed to the formation of an electron-rich space charge in front of the probe [10, 12]. The experimental result in this paper is in agreement, however, with another study on a magnetized low-temperature plasma, where the floating potential measured with emissive and plugged probes turned out to be very similar [17]. One reason for the different conclusions on this kind of comparisons might be the plasma parameters. Maybe a deviation of the emissive floating potential from the plasma potential is more relevant to

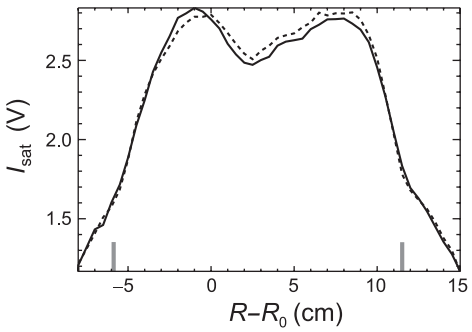

Figure 3. Influence of the emissive probe on the plasma equilibrium. Radial profiles of the ion saturation current in argon from the central tip of the transport probe for cold (——) and emissive (- - - -) outer probes (#2189). The position of the separatrix is marked by grey bars.

high-temperature plasmas than for plasmas with a characteristic electron temperature of 10 eV. Such an investigation should be subject of further comparative studies.

A current of $I_H \approx 2.3$ A yields a symmetric characteristics, i.e. the currents in the ion and electron saturation regimes are approximately equal. This condition is a reasonable and commonly used compromise between small errors in the potential measurement, a long lifetime of the probe and small errors due to a virtual cathode establishment in front of the probe, which can become a problem for very high emission currents [12]. As seen in figure 2, due to the strong dependence of the Richardson emission on temperature, one has to be careful that the heating current does not fall below a critical value. The second derivative of the cold characteristics does not show a clear deviation of the electron distribution function from a Maxwellian.

Emissive probes are very fragile but they also have a number of advantages. The acquisition of the floating potential of an emissive probe is simple and fast. In addition, due to a symmetric characteristics, the impendency of a floating emissive probe is much lower than that of a floating Langmuir probe.

When the heating system is fully disconnected from the probe, the tips can be used as Langmuir probes. This makes it possible to get direct comparisons between potential measurements with a Langmuir and a hot, emitting probe. The term ‘cold probe’ will be used for the emissive probe when it is not heated and therefore acts as a Langmuir probe. It has been carefully checked that the loop geometry of the cold probe gives the same results as a cylindrical probe. Probe data have been taken over the entire poloidal plasma cross-section for time intervals of 64 ms at a rate of 2 MHz.

3. Equilibrium profiles

Before investigating fluctuations and transport, attention is drawn to equilibrium profiles of potential and density. Radial profiles of the potential and the ion saturation current $I_{i,sat}$ have been measured with both the cold and the emitting probes.

Figure 3 shows the influence of the electron emission from the two outer probes on ion saturation current measurements carried out with the central probe. The agreement of the two profiles measured with the outer probes cold and emissive is excellent. Hence for a probe separation of 7.5 mm there is no limitation in using Langmuir probes in the vicinity of an emissive probe.

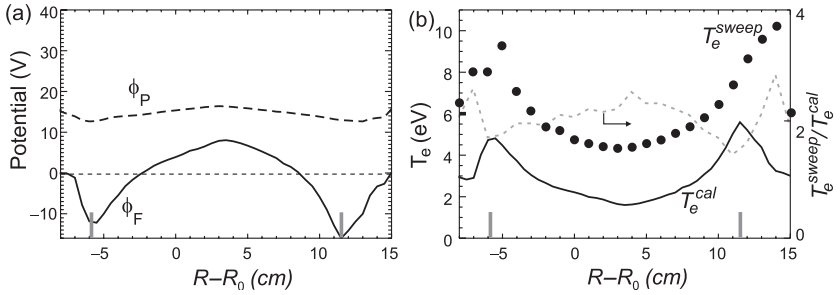

Figure 4. (*a*) Radial potential profiles measured with cold (——) and emitting probes (- - - -) (#2189). The floating potential shows a pronounced minimum in the region of the separatrix marked by grey bars. (*b*) Electron temperature profile T_e^{cal} computed using equation (4) from a simultaneous measurement with one cold and one emitting probe (——) compared with a profile T_e^{sweep} from probe characteristics (●●●●). The temperature measurements are from a different discharge at the same nominal parameters. The dashed line gives the ratio between measured and estimated temperatures.

Figure 4 depicts a comparison of potential measurements carried out with the same probe, once operated cold and once emissive. The floating potential is more negative compared to the plasma potential. It assumes strong negative values in the region of the separatrix at $R - R_0 \approx 12$ cm, where the electric field reverses sign. The plasma potential is smoother with only a small dip at the separatrix. Using simple probe theory, from the two profiles the electron temperature profile can be deduced. For Maxwellian plasma, floating and plasma potential are related by the expression [18]

$$\Phi_F = \Phi_P - \frac{T_e}{e} \ln\left(\frac{S_e}{S_i}\frac{(1-\gamma_e)}{(1+\gamma_i)}\frac{j_{e,sat}}{j_{i,sat}}\right), \tag{3}$$

where $j_{i,sat} = 0.61en\sqrt{T_e/m_i}$ and $j_{e,sat} = en\sqrt{T_e/2\pi m_e}$ are the current densities for ions and electrons, respectively, $\gamma_{i,e}$ the respective secondary emission coefficients and $S_{i,e}$ the effective collecting areas, $m_{i,e}$ the masses and e the elementary charge. The expressions apply for the plasma in TJ-K with single charged, cold ions (<1 eV). The collecting areas for electrons and ions can differ. In a magnetized plasmas as the present one, with ion gyro radii larger than the probe loop, the calculation of S_i is not a simple task [19]. If electrons are magnetized and ions unmagnetized, a ratio of $S_e/S_i = 2/\pi$ can be deduced [10]. In cases where $S_i = S_e$ and $\gamma_i = \gamma_e = 0$ is valid, the equation reduces to

$$e(\Phi_P - \Phi_F) = \frac{(6.7 + \ln A_i)}{2} T_e, \tag{4}$$

where A_i is the atomic mass number (40 for argon). Since Φ_P and Φ_F have been measured, the equation can be used to calculate the electron temperature. This has been done with the data of figure 4(*a*). In figure 4(*b*), the obtained radial temperature profile is compared with temperatures measurements deduced from swept Langmuir probe characteristics, which have been carried out on another discharge at the same nominal parameters. These temperatures have been derived from the exponential region of the characteristics restricted to a range up to about T_e/e above the floating potential. Different upper limits have been checked to yield the same temperature values. The two temperature profiles in figure 4(*b*) deviate by an almost constant factor of about 2.

In order to compare this factor with previous results from one-point measurements in the CASTOR tokamak plasma with hot hydrogen ions [10], the factor $\Delta = e(\Phi_P - \Phi_F)/T_e$ is introduced. The simple expression (4) yields for an argon plasma $\Delta^{cal} = 5.2$. If the measured

potentials and temperatures (T_e^{sweep}) are used, the factor decreases to $\Delta^{sweep} = 2.6$. Hence the ratio is $\Delta^{cal}/\Delta^{sweep} = 2.0$. This confirms the trend reported from CASTOR, where the ratio was 1.5. It should be noted, however, that in [10] the expression for $j_{i,sat}$ was used without the Bohm factor of 0.61. If this factor is included, the value changes from $\Delta^{cal}/\Delta^{sweep} = 1.5$ to 1.2.

According to equation (3), this ratio can be interpreted by differences in secondary electron-emission coefficients or effective collecting areas between electrons and ions. In order to reproduce the measured electron temperature, the effective probe surface for the ions needs to be 14 times larger than that of the electrons, which is an unrealistic value. Also a needed value of $\gamma_i \approx 13$ is not realistic. Hence similar as in [10], there is no simple explanation of this difference. However, since the ratio $\Delta^{cal}/\Delta^{sweep}$ is almost constant across the plasma radius, explanations depending on the local density or electron temperature are ruled out. Since the magnetic field changes by a factor of 2 across the scanned range, the ion gyro radius also cannot be used as the leading parameter to account for this difference.

4. Fluctuation and transport measurements

Also, for the same discharges as used for the equilibrium profiles, full sets of fluctuation data are available. Therefore, all data were consistently taken for two discharges, one measured with emitting and the other with cold probes. The probability density functions (PDFs) of density and potential fluctuations depend on the radial position. For the two cases of cold and emitting outer probes, figure 5 shows the PDF of ion saturation current fluctuations measured with the central probe at two different radial positions (left-hand side) and the dependences of the moments of the PDF, which are the standard deviation, the skewness and the kurtosis, on radius (right-hand side). The comparison shows that emissive probes operated at a distance of 7.5 mm from a Langmuir probe do not substantially influence ion saturation current measurements carried out with the latter. This holds for both equilibrium and fluctuation measurements and is an important finding for the use of emissive probes in our system, since for the investigation of turbulent transport potential and saturation current have to be measured in close vicinity.

The turbulent transport fluctuations have been computed according to equation (1). The poloidal electric field at the position of the central probe is deduced from the difference of the potentials measured with the two outer probes. The results obtained with cold and emitting outer probes are compared. Figure 6(*a*) is devoted to the dc values while the standard deviation of the fluctuations can be found in figure 6(*b*).

Compared to the radial gradient of the floating and plasma potentials, which are of the order of $200\,V\,m^{-1}$ for Φ_F and $40\,V\,m^{-1}$ for Φ_P (see figure 4), the values of the poloidal gradients are smaller with values $<100\,V\,m^{-1}$ and $<10\,V\,m^{-1}$, respectively. The deviation of the poloidal gradient from zero can be attributed to misalignment of the probes on the flux surface so that they pick up a contribution from the radial component. The strongest deviations are in the region of the separatrix, where the radial gradient is largest. The fluctuations in the poloidal gradient, which are the poloidal electric field fluctuations in figure 6(*b*), on the other hand, show rather good agreement.

A further important quantity for turbulent transport is the cross-phase between density and potential fluctuations. The relevant parameter is the cross-phase frequency spectrum $\alpha(f)$, which has to be regarded in context with the coherency spectrum $\gamma(f)$ between both signals [20]. Only in the frequency domain where the signals are coherent, the cross-phase determines the magnitude and the direction of transport. The cross spectrum shows strong variations with the radial position.

Figure 7(*a*) depicts coherence and phase spectrum in the density gradient range at the position of $R - R_0 = 10\,cm$. Again, all quantities were calculated for cold (solid lines)

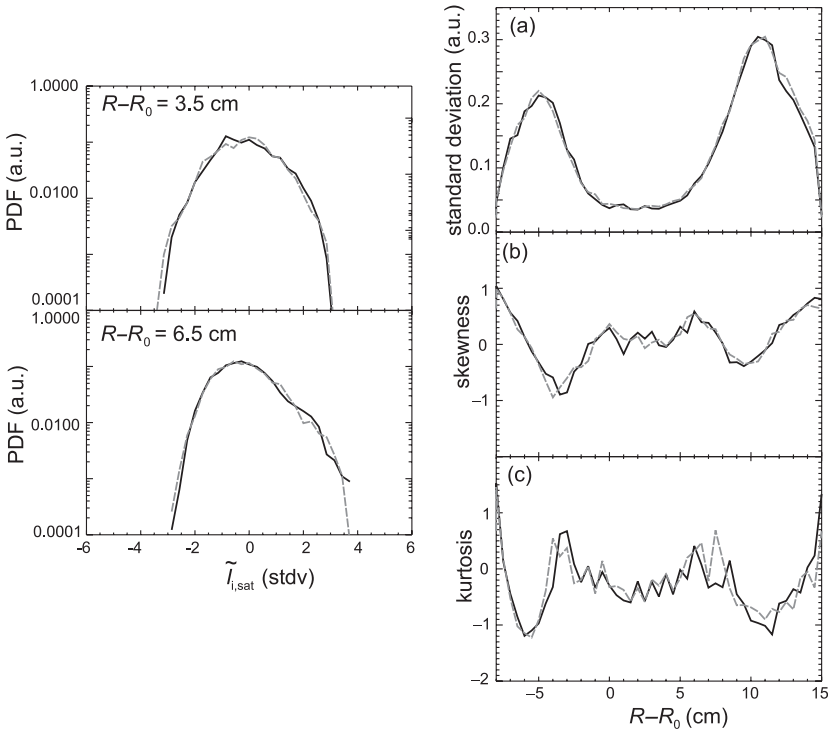

Figure 5. Influence of the emissive probe on plasma fluctuations. Left: comparison of the PDFs of $I_{i,sat}$ fluctuations measured with the central probe for the cases of cold (——) and emitting (- - - -) outer probes measured at the radial positions $r = 3.5$ and $r = 6.5$ cm. Right: dependence of the moments of the PDFs of $I_{i,sat}$ fluctuations on radius. The figures show the standard deviation (a), the skewness (b) and the kurtosis (c).

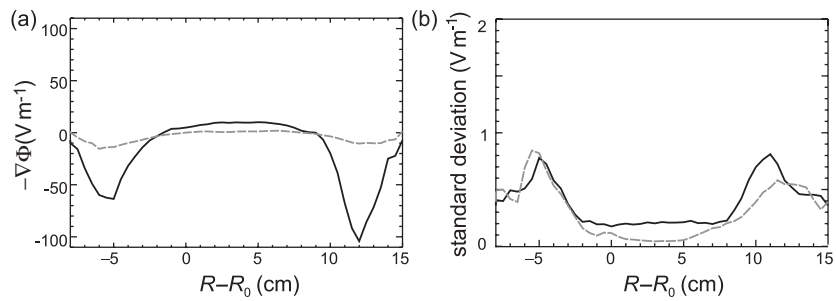

Figure 6. Poloidal gradient of the potentials measured with the two outer probes which measured the floating potential (——) or the plasma potential (- - - -). (*a*) Shows the dc component and (*b*) the standard deviation of the fluctuations (#2189).

and emissive (dashed lines) outer probes. Excellent agreement is found for the two different measurements. The coherency is reasonably large for the low-frequency range $f < 20$ kHz and the cross-phases are close to zero as also measured previously in wave-number space [21]. The coherency of the cold-probe measurements is somewhat lower for frequencies above 7 kHz. In the range $f > 20$ kHz, the coherency decreases strongly for two measurements, resulting in a higher uncertainty of the cross-phase.

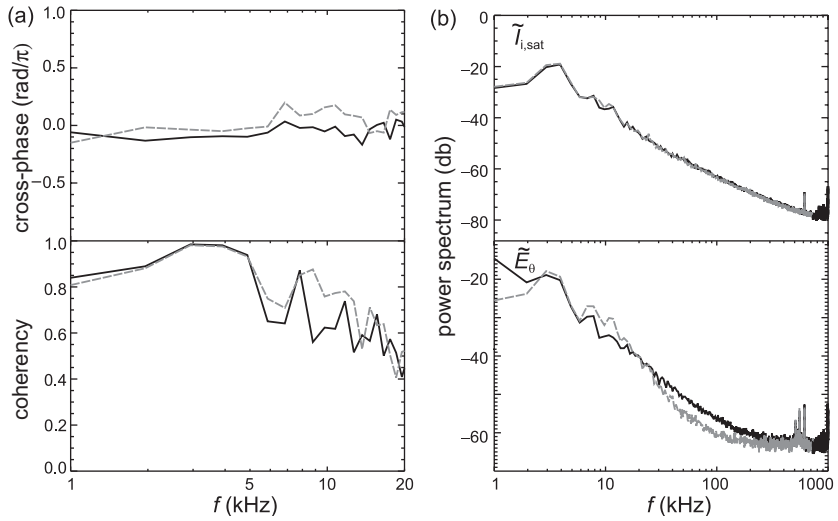

Figure 7. (*a*) Cross-phase and coherency spectra between density and potential fluctuations where the potential was measured with cold (——) and emissive (- - - -) outer probes. (*b*) Power spectra of ion saturation current (upper) and poloidal electric field fluctuations (lower) for cold (——) and emissive (- - - -) probes.

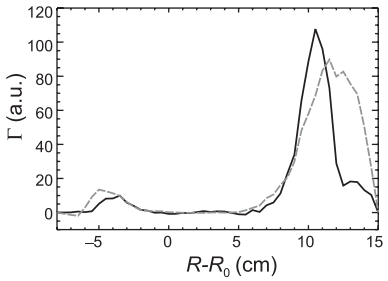

Figure 8. Radial profile of the mean turbulent transport measured with cold (——) and emitting probes (- - - -). For both curves, the density has been measured with the same probe and both curves have been normalized with the same factor. Hence, the comparison is quantitative.

Figure 7(*b*) shows the corresponding power spectra of ion saturation current and poloidal electric-field fluctuations. The spectra are averaged over 32 realizations of 2048 data points each. Also, the agreement of the power spectra measured with cold an emissive probes is very good. The spectra of poloidal electric field computed from floating potential and plasma potential fluctuations are very similar. This shows again that the influence of the emitted electrons on the ion saturation current fluctuations is marginal.

Finally, figure 8 shows the radial turbulent transport profile evaluated from the data discussed above. The qualitative agreement is satisfactory in the sense that the reproducibility of such complex measurements is not perfect, especially if emissive probes are involved. In addition, the main discrepancy appears outside the last flux-surface at $R - R_0 \geqslant 12\,\mathrm{cm}$. Transport is largest in the region of the density gradient and is small in the centre of the plasma where the density gradient vanishes. The largest value is found on the low-field side.

These results show that, at least for plasmas at the parameters in TJ-K, the use of Langmuir probes is justified for the investigation of potential fluctuations.

5. Summary and conclusion

Measurements of radial turbulent transport and related quantities were carried out with a conventional transport probe and a transport probe equipped with two emissive probes. In contrast to the conventional probe, where the poloidal electric field fluctuations are estimated from the floating potential, the emissive probes measure plasma potential fluctuations. The main objective of the study was to investigate whether in turbulence studies it is sufficient to use the floating potential from Langmuir probes or whether the plasma potential from the more complicated emissive probes has to be used. The dc potentials from the two probes are, of course, different, but it has been demonstrated that the fluctuating components measured with the two probe systems and derived quantities agree rather well.

The differences in the equilibrium values of floating and plasma potential were found to be larger than expected from simple probe theory, i.e. the deviations were larger than estimated from equation (4) with the measured electron temperature profile. This is consistent with results from the edge plasma of the CASTOR tokamak [10] and is also consistent with previous studies on TJ-K [22]. Since the difference is approximately constant across the plasma radius, explanations depending on the local density, electron temperature or ion gyro radius are ruled out. One possible explanation is a higher effective collection area for the ions. Detailed simulations of the orbits of gyrating ions around the probe are needed to address this problem. From the comparison, however, the effective ion collecting surface needs to be 14 times larger than that of the electrons, which is an unrealistic value. A similar statement is true for the secondary electron-emission coefficient where one needs a value of $\gamma_i \approx 13$. Recently, data from the stellarator W7-AS have been analysed, where the same kind of analyses produced agreement with probe theory [23]. Since there is an order of magnitude increase of magnetic field strength from TJ-K to CASTOR and W7-AS, the magnetization of the ions could be important. On the other hand, the magnetic field in TJ-K changes across the radius by a factor of two while the measured correction factor stays constant.

In contrast to the dc values, the potential fluctuations measured with cold and emitting probes have very similar properties. Power spectra, the PDF and the moments of the PDF resulting from cold and emissive probes agree very well. The cross-phases between the two potential measurements with the ion saturation current are close to zero for all radial positions. This is in agreement with drift wave dynamics found in previous work on turbulent transport and coherent structures in TJ-K [15,21] and with simulation results given in [24,25]. The turbulent transport measured with the transport probe shows the same radial dependence independently of whether floating or plasma potential is measured.

As a byproduct, this study showed that there is only little influence of emissive probes on Langmuir probes operated in close vicinity. The inspected ion saturation current data from the Langmuir probes was not altered when an emissive probe was operated at a poloidal distance of 7.5 mm. Mean values, moments of the PDF and power spectra were almost identical when the adjacent probes were operated cold or emissive. Hence, emissive probes can be operated together with Langmuir probes without a visible drawback for the latter.

It should be pointed out that there is strong practical interest in using Langmuir instead of emissive probes. Langmuir probes have a much simpler design and an almost unlimited lifetime. Emissive probes are extremely fragile with a lifetime in TJ-K of at best 2 h. The actual state of emissive probes has to be checked frequently and for optimal results, the heating current has to be adjusted to the plasma parameters. Furthermore, the background noise level rises due to additional power supplies and wiring. It turned out to be rather tedious to measure a complete set of reliable radially resolved data. In addition, for multi-probe measurements with up to 64 probes as used in [21] it is virtually impossible to use emissive probes.

In conclusion, for the plasma parameters of the torsatron TJ-K the fluctuations in plasma and floating potential have very similar statistical properties. Hence, it is possible to carry out turbulence studies with Langmuir probes only and to interpret floating potential as plasma potential fluctuations. Therefore, this study provides the basis for the use of multi-probe arrays which in practice can be built with Langmuir probes only.

Acknowledgments

Financial support by Max-Planck-Institut für Plasmaphysik, Garching is gratefully acknowledged. The TJ-K device was provided by CIEMAT, Madrid.

References

[1] Zweben S J and Gould R W 1985 *Nucl. Fusion* **25** 171
[2] Ritz C P *et al* 1989 *Phys. Rev. Lett.* **62** 1844
[3] Endler M *et al* 1995 *Nucl. Fusion* **35** 1307
[4] Hidalgo C 1995 *Plasma Phys. Control. Fusion* A **37** 35
[5] Grulke O, Klinger T, Endler M, Piel A and the W7-AS Team 2001 *Phys. Plasmas* **8** 5171
[6] Lechte C, Niedner S and Stroth U 2002 *New J. Phys.* **4** 34
[7] Pfeiffer U, Endler M, Bleuel J, Niedermeyer H, Theimer G and the W7-AS Team 1998 *Contrib. Plasma Phys.* **38** 134
[8] Hershkowitz N, Nelson B, Pew J and Gates D 1983 *Rev. Sci. Instrum.* **54** 29
[9] Ono S and Teii S 1979 *Rev. Sci. Instrum.* **50** 1264
[10] Schrittwieser R *et al* 2002 *Plasma Phys. Control. Fusion* **44** 567
[11] Balan P *et al* 2003 *Rev. Sci. Instrum.* **74** 1583
[12] Ye M Y and Takamura S 2000 *Phys. Plasmas* **7** 3457
[13] Krause N, Lechte C, Stroth U, Niedner S, Ascasibar E and Alonso J 2002 *Rev. Sci. Instrum.* **73** 3474
[14] Mahdizadeh N, Stroth U, Lechte C, Ramisch M and Scott B 2004 *Phys. Plasmas* **11** 3932
[15] Stroth U, Greiner F, Lechte C, Mahdizadeh N, Rahbarnia K and Ramisch M 2004 *Phys. Plasmas* **11** 2558
[16] Siebenforcher A and Schrittwieser R 1996 *Rev. Sci. Instrum.* **67** 849
[17] Greiner F, Block D, Piel A, Ratynskaja S, Helblom G and Rypdal K 2003 *Plasma Physics: 11th Int. Congr. on Plasma Physics (ICPP2002)* (New York: AIP) **669** 64
[18] Chen F 1965 *Phys. Fluids* **8** 912
[19] Demidov V I, Ratynskaia S V and Rypdal K 2002 *Rev. Sci. Instrum.* **73** 3409
[20] Powers E J 1974 *Nucl. Fusion* **14** 749
[21] Lechte C 2003 Microscopic structure of plasma turbulence in the torsatron TJ-K *PhD Thesis* Christian-Albrechts-Universität, Kiel
[22] Rahbarnia K *et al* 2003 *Proc. 14th Int. Stellarator Workshop (Greifswald)*
[23] Fink M A and Klinger T 2004 *Contrib. Plasma Phys.* **44** 668
[24] Scott B 1997 *Plasma Phys. Control. Fusion* **39** 471
[25] Niedner S, Scott B D and Stroth U 2002 *Plasma Phys. Control. Fusion* **44** 397